Experimental and *ab initio* determination of the bending potential of HCP

Kevin K. Lehmann[a)]
Department of Chemistry, Harvard University, Cambridge, Massachusetts and George R. Harrison Spectroscopy Laboratory, M.I.T., Cambridge, Massachusetts

Stephen C. Ross
Department of Chemistry, University of Alberta, Edmonton, Alberta, Canada

Lawrence L. Lohr
Department of Chemistry, University of Michigan, Ann Arbor, Michigan

(Received 4 December 1984; accepted 1 February 1985)

The emission properties of HCP excited to the A, B, and d electronic states have been studied. Lifetimes and quenching rates have been measured. By spectrally resolving the emission spectrum, the energy of 94 vibrational levels of the ground electronic state have been measured to an accuracy of $\approx 5\ cm^{-1}$. These energy levels were fit to experimental accuracy by a rigid bender Hamiltonian thereby determining the bending potential over a range of bending angle from 0 to 100° (0–17 500 cm^{-1}). An *ab initio* bending potential has been computed for HCP and found to be in excellent agreement with the experimentally fitted one over the range that the experimental data span. This potential predicts that HPC has an energy maximum with respect to the bending coordinate. The bending potential decreases monotonically by about 30 000 cm^{-1} in going from HPC to HCP.

INTRODUCTION

HCP is an obscure molecule to most chemists, yet it is well characterized spectroscopically. In fact, more electronic states have been characterized for HCP than for any other polyatomic molecule.[1] This was reported in one paper by Johns, Shurvell, and Tyler.[2] This work was extended by Hartford *et al.*[3] who used optical stark spectroscopy to measure the dipole moment for several excited electronic states. Frost *et al.* have measured the photoelectron spectrum of HCP,[4] and King *et al.*, the emission spectrum of the HCP^+ ion.[5] The ground electronic state has been thoroughly studied as well. The microwave spectrum was studied by Tyler[6] and by Johns, Stone, and Winnewiser.[7] Cabana and coworkers[8–11] have used high resolution IR spectra of HCP and its common isotopically substituted species to determine most of the harmonic and second order anharmonic constants. In contrast to this extensive spectroscopic information, there exists no thermochemical data on HCP, so its dissociation energy is not yet known.

The known spectroscopic properties of HCP are very similar to those of HCN. Like HCN, the ultraviolet absorption spectrum is dominated by a bent(A)←linear(X) transition.[2] For HCP, the origin for this transition is at 2874.22 Å, which is much more accessible than the $A \leftarrow X$ system of HCN.[12] The absorption spectrum of HCP does not show the diffuseness that characterizes the HCN spectrum, but it is not known if this is because the transitions are below the dissociation limit or not.

It is known that the bending potential of HCN has a well on the HNC side $\sim 5200\ cm^{-1}$ higher than the HCN side.[13] *Ab initio* calculations put the barrier to isomerization at 17 500 cm^{-1}.[14] The present work was undertaken to characterize the bending potential of HCP to see if it has analogous behavior. Because of the bent←linear nature of the $A \leftarrow X$ transition, the fluorescence spectrum was expected, and found, to have a long progression in the bending mode. Because the C–P bond length also changes, the C–P stretch is also active in fluorescence. No observable activity in the C–H stretch was found.

From the resolved fluorescence spectrum, 94 vibrational energy levels have been observed in the ground electronic state. These states have up to 27 quanta in the bending mode and up to five quanta in the C–P stretching mode. Most of these observed levels are reported for the first time. These energy levels are fit, to within experimental accuracy of 5 cm^{-1}, by a rigid bender Hamiltonian[15–17] with five free parameters. The bending potential can be considered to be determined over a range of bond angles corresponding to the classical turning points of the highest observed bending state 0–100°(0–17 500 cm^{-1}). The slope of the bending potential is still increasing at the highest observed level so the potential shows no sign of turning over, like the HCN potential does in this energy region.

An *ab initio* bending potential for HCP has been calculated at the MP4/31G** level (fourth order Møller–Plesset perturbation theory) using bond lengths optimized at the HF/6-31G* level for a given HCP bond angle. The calculated bending potential is in excellent agreement with the experimentally determined one over the experimentally sampled region. The *ab initio* potential predicts that HPC is approximately 30 000 cm^{-1} higher in energy than HCP, and has a maximum in the bending potential. This is in sharp contrast to the HCN behavior.

EXPERIMENTAL

HCP was synthesized by the procedure of Hopkinson *et al.*[18] who first showed how to generate approximately pure samples of HCP. Briefly, CH_3PCl_2 was pyrolyzed in a quartz

[a)] Junior Fellow, Harvard Society of Fellows.

 0021-9606/85/104460-10$02.10

capillary tube, 30 cm long, heated to greater than 1000 °C. The major products of the pyrolysis are HCl, HCP, and CH_4. The HCl and low volatile products are trapped in a KOH filled trap, cooled to dry ice temperature. The HCP and unreacted CH_3PCl_2 is trapped at 77 K, the CH_4 is pumped away. When the 77 °K trap is warmed to 135 °K, the HCP comes off with a vapor pressure of a few Torr. It can then be stored indefinitely in a glass tube at 77 °K. When exposed to glass, the HCP is quite stable at room temperature as long as the pressure remains below a few Torr.

HCP fluorescence was observed by exposing it to the frequency doubled output of a dye laser pumped by the second harmonic output of a YAG laser. The sample was exposed to ~0.25 mJ of UV at a repetition rate of 20 Hz. The HCP was found to be photochemically unstable when pumped to the excited electronic state, so it was necessary to slowly flow the HCP through the fluorescence cell. In all the measurements reported here, the dye laser was operated with a linewidth of ~0.3 cm^{-1} and was tuned to the R branch band head of different vibrational states. One band, the B–X transition which has its R branch bandhead 2782.22 Å, was examined with rotational resolution and the lifetime found not to depend noticeably on J over the range $J = 1$–9.

The optical setup is shown in Fig. 1. Undispersed fluorescence was detected to aid in tuning to the R branch heads, as well as to monitor the HCP concentration. Fluorescence was dispersed through a Spex 1 m double monochronometer using a grating with 1200 grooves/mm and blazed at 1 μ. Filters were used to separate the overlapping orders of the monochrometer. The light was detected by a photomultiplier tube which has an extended S-20 cathode. Light from a Ne hollow cathode lamp was focused through the cell and onto the slits of the monochrometer providing calibration lines. The grating drive proved stable over a period of several months, so a single calibration scan, performed with narrow slits, was used.

For the lifetime measurements, the signal from the PMT collecting the undispersed fluorescence was captured on a Tektroniks transient digitizer and averaged on a DEC MINC computer. The lifetimes were determined by a least squares fit of the decay curves. Both the data acquisition and analysis programs were supplied by Patrick Vaccaro of MIT. The HCP pressure was monitored by a thermocouple gauge, which was calibrated for use with HCP by comparison with a capacitance manometer.

In recording the dispersed fluorescence, the output of the PMT was detected with a boxcar averager. The gate width was set at several μs. The HCP pressure (≈100 mTorr) was high enough that the fluorescence was collisionally quenched. Despite this, the qualitative features of the spectrum appeared to be independent of gate width on the boxcar, indicating that collisionally relaxed fluorescence was not important.

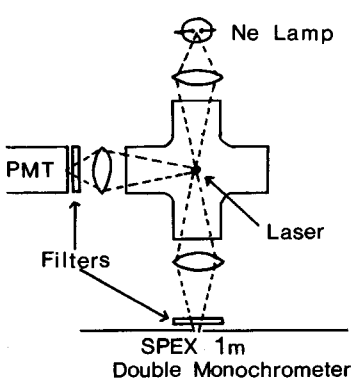

FIG. 1. Optical setup. Frequency doubles output from YAG pumped dye laser propagates vertically out of the page.

TABLE I. Lifetime measurements of HCP.

λ	Assignment	Decay rate (MHz)	Quenching rate (MHz/Torr)
2874.82 Å	$A\ 00^10 \leftarrow 000$	0.46 ± 0.07	...
2870.99 Å	$A\ 01^20 \leftarrow 01^10$	0.36	15
2848.12 Å	$A\ 02^00 \leftarrow 01^10$	0.36	15
2844.65 Å	$A\ 00^21 \leftarrow 01^10$	0.60	15
2835.48 Å	$A\ 01^31 \leftarrow 02^20$	0.53	15
2825.72 Å	$A\ 01^10 \leftarrow 00^00$	0.64	9
2820.90 Å	$A\ 02^20 \leftarrow 01^10$	0.53	9
2808.26 Å	$A\ 01^01 \leftarrow 01^10$	0.48	14
2785.53 Å	$A\ 02^10 \leftarrow 000$	0.16	14
2782.22 Å	$B\ 00^10 \leftarrow 000$	0.18	14
2777.58 Å	$d\ 00^10 \leftarrow 000$	0.53	7
2772.05 Å	$A\ 02^01 \leftarrow 01^10$	0.47	4
2771.51 Å		0.46	8
2770.49 Å	$A\ 00^22 \leftarrow 01^10$	0.76	13
2751.67 Å	$A\ 01^11 \leftarrow 00^00$	0.37	14
2748.35 Å	$A\ 02^21 \leftarrow 01^10$	0.37	15
2740.15 Å	$A\ 03^10 \leftarrow 00^00$	0.40	...
2735.74 Å	$A\ 01^02 \leftarrow 01^10$	0.62	12

PHOTOCHEMICAL ACTIVITY

The HCP sample was found to decompose with a time constant of about 5 min when exposed to the 20 Hz laser excitation (≈250 μJ/pulse) at pressures (≈100 mTorr) where the upper electronic state was largely collisionally quenched. The decomposition ceased or at least slowed drastically when the laser was blocked. The vapor pressure of the sample did not change, even when almost all the HCP had been destroyed. If our sample was predominantly HCP,[18] this implies that one molecule of gas was made for each HCP molecule destroyed. The rapidity of the photodecomposition implies that the quantum yield for HCP destruction must be on the order of unity, unless a chain reaction is initiated photochemically.

LIFETIME RESULTS

The measured radiative and collisional decay rates of the accessible vibrational bands of HCP are listed in Table I. The assignment for the bands is taken from Johns *et al.*[2] The decay curves were adequately fit by a single exponential decay. No evidence of quantum beats was found in the decay curves. The measurement of the radiative decay rates required working at very low pressures (a few mTorr). It was difficult both to maintain stable pressure and obtain accurate pressure readings, so the radiative decay rates are only accurate to about 25%. Despite this, several qualitative observations can be made. The apparent erratic variation of decay rate with vibrational state of the A state is consistent with Johns *et al.*'s observation of a large number of discrete

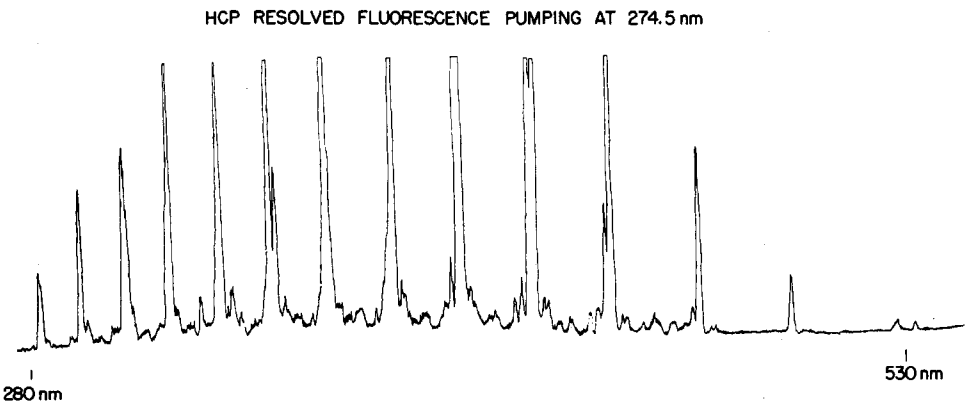

FIG. 2. Low resolution resolved fluorescence spectrum of HCP, pumped at 2745 Å.

perturbations in the spectrum. The weak variation of decay rate with vibrational energy of the A state argues that nonradiative decay is not important, i.e., the zero pressure decay rate is in fact the radiative rate. The fluorescence properties of the B and d states are very similar to those of the A state. This supports Johns *et al.*'s conjecture that these states gain their intensity by borrowing from the A state. The quenching rate of 15 MHz/Torr is comparable to rotational relaxation rates, and explains why collisionally relaxed fluorescence was not a problem.

RESOLVED FLUORESCENCE

Figure 2 shows a low resolution plot of the spectrally resolved fluorescence spectrum of HCP, pumping at 2745 Å. A long progression of 14 members can be seen. Not evident from the linear wavelength scale is the very harmonic spacing of the progression, with the spacing between the first two members being only about 10% more than the spacing of the last two members. This is quite surprising since the 13th member of the progression has about 17 000 cm^{-1} of excitation energy. The spacing of the progression, about 1300 cm^{-1}, is indicative of either C–P stretching excitation (ν_3) or even quanta of the bending mode (ν_2). No progression built upon the C–H stretch (ν_1) could be assigned. The same qualitative spectrum was observed when pumping different vibrational energy levels of the A state, as well as when pumping the B and d states. As will be shown below, the long progression is primarily in the bending mode. The B and d states are assigned as linear excited electronic states. Thus the fact that they give the same fluorescence spectrum as the strongly bent A state is further evidence that they are fluorescing and presumably also absorbing by borrowing A state character.

Emission spectra from two excited states were studied at high resolution. The first we will discuss is from the A $(0,2^0,1)$ energy level, pumped with the hot band transition at 2772.05 Å. The superscript refers to the K value of the state. The dye laser was set to excite the R bandhead. This excites principally R (6), though R (5) and R (7) are excited as well. Because of the selection rules for a perpendicular transition, the fluorescence from $K = 0$ can only terminate on $K = l = 1$ in the lower state. The rotational selectional rules predict a P, Q, and R branch in emission (intensity of about 1:2:1), separated by approximately 2 B J which is about 10 cm^{-1} for the J values being pumped. The resolution was not high enough to resolve the P, Q, R structure, so emission bands were identified by the stronger, central Q branch. This final state has one more unit of rotational angular momentum than the initial state (we are pumping an R branch) and so included with the vibrational energy, there is about 2 B J more rotational energy than in the initial state. Therefore, in computing the vibrational energy from the difference between pump and emission energy, 10 cm^{-1} was subtracted to compensate for this extra rotational energy. The energy of the $(0,1^1,0)$ state, the lower level of the pump transition, was taken from Garneau and Cabana.[10] Figure 3 shows a high resolution scan of the first member of the progression. The two observed states, $(0,3^1,0)$ and $(0,1^1,1)$, were both known from IR work, and so assignment was straightforward. In extending to higher members of the progression, the fine structure gets more complicated, as shown in Fig. 4, which shows the eighth member of the progression. The lower members of the progression were assigned using Cabana *et al.*'s anharmonic constants.[11] After assigning the lower energy levels in this way, three third order anharmonic constants were fit to the data, and used to extrapolate to higher energy. In this bootstrap method, most of the strong features in the spectrum were assigned, though several notable exceptions remain, one being the unassigned peak in Fig. 4. The resulting spectroscopic constants (ω_i and x_{ij} from Cabana *et al.*, y_{ijk} fitted to the data) reproduced the observed vibrational energy levels (rms deviation of 8 cm^{-1}) to about the experimental precision, believed to be about 5 cm^{-1}. However, there were clearly systematic trends in the residuals. Further, the y_{ijk}'s were highly correlated with the assumed

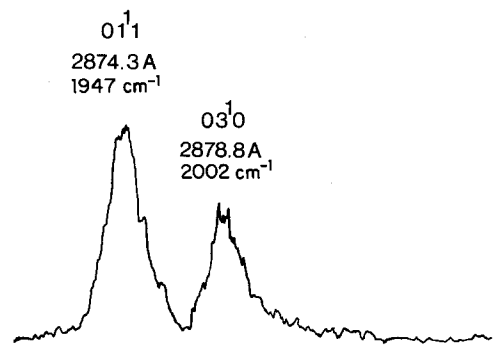

FIG. 3. High resolution scan of first member of progression. Pumping wavelength is 2772.05 Å. Frequency gives vibrational energy of final state, relative to the ground vibrational state.

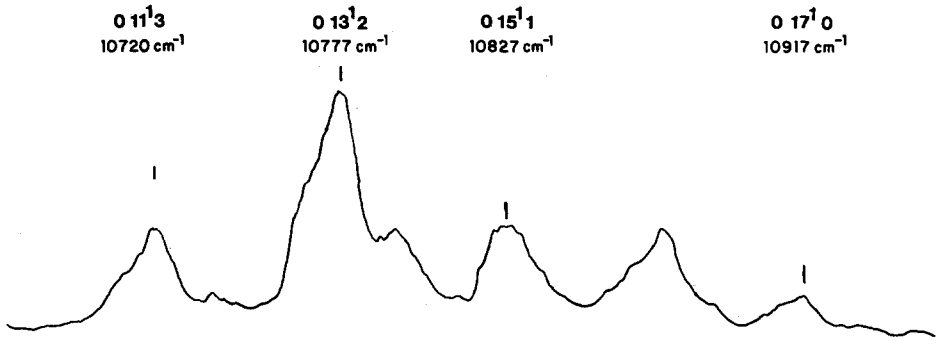

FIG. 4. High resolution scan of eighth member of the progression.

constants, and gave no physical insight into the molecule.

The 40 assigned energy levels were fit to a physical Hamiltonian, the rigid bender Hamiltonian, which will be discussed in the next section. In addition to determining the bending potential of HCP, the results of the fit were used to predict the energies of $l = 0$ and 2 vibrational states without extra parameters.

The other high resolution spectrum examined is from the B state origin at 2782.22 Å. This state was assigned by Johns *et al.* as a $^1\Pi$ electronic state, but Moehlmann *et al.* reassigned it as $^3\Delta_1$ based upon its Zeeman effect.[19] We assign its intensity as coming from the A state, most probably from the nearby $(0,2^1,0)$ vibrational state. The radiative lifetime was found not to vary over the range $J = 1$–9, indicating that the mixing with the A state is not caused by rotational interactions. The selection rules for fluorescence from this $K = 1$ state are to states with $l = 0$ and 2. The separation in energy between these states should be about $4g_{22}$ which is about 20 cm^{-1}. When pumping on an R branch transition, the rotational selection rules give a P and R branch in emission, but no Q branch (for $l = 2$ the Q branch is not completely forbidden, but much weaker). Thus the P, R doublets are also expected to be about 20 cm^{-1}, leading to a complicated spectrum. Figure 5 shows the first member of the progression, with the vibrational assignments marked. As can be seen, the spectrum is badly overlapped. Initially, it proved difficult to assign the bulk of the spectrum, especially since there was no information on how g_{22} would vary with vibrational quantum numbers. Since for a linear molecule basis, states with the same vibrational quanta, but different values of l correlate in a nonlinear molecule to different vibrational states with different values of K, it was expected that g_{22} would vary quite significantly with bending quantum number. Therefore, initially only the lowest states could be assigned with any confidence. The rigid bender predictions were used to assign the spectra, and the predicted energy levels agreed to almost identical error as those $l = 1$ levels that were initially fit, despite the problems of blending in the $l = 2$ spectrum. As it turns out, for the highest observed bending levels, g_{22} increases by only 50%. Combining the results from the two upper states, 94 vibrational energy levels were measured, relative to the ground vibrational state. Most of the states have never been observed before. The experimental accuracy is not very high, but it is probably only about five times worse than the believed accuracy of the Hamiltonian used, and is more than sufficient to determine the bending potential to chemically interesting accuracy.

A few final comments about the emission intensities are in order. In a mixed progression such as observed for HCP, with both ν_2 (bending mode) and ν_3 (C–P stretch) active, one expects the highest observed energy levels to be states with both ν_2 and ν_3 excited. Figure 6 shows the highest observed level, $(0,27^1,0)$. The state $(0,25^1,1)$ should appear to the left of the $(0,27^1,0)$ state, but nothing is observed on that side. The weak peaks on the high frequency side appear in many of the high energy spectra, and are not assigned. The intensity of the ν_3 excited progressions just die away before the pure ν_2 progression. Exciting to higher A state vibrational energy levels would presumably move the Franck–Condon factors

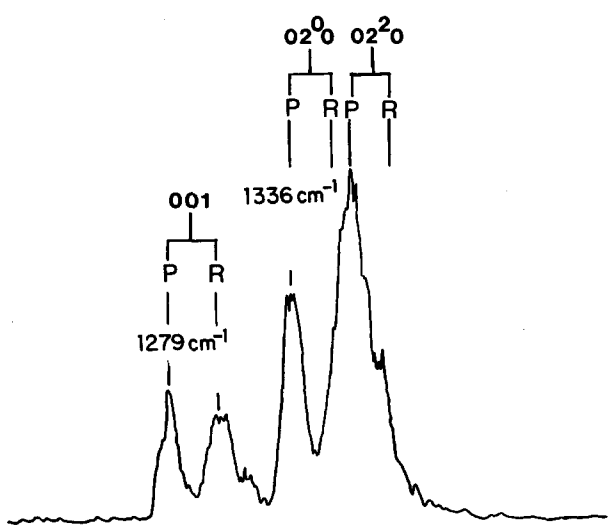

FIG. 5. High resolution scan of the first member of the progression pumping at 2782.22 Å.

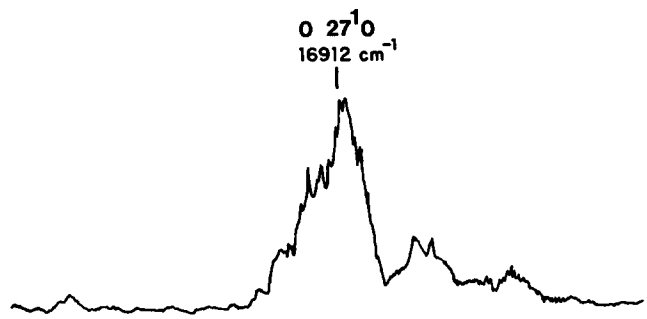

FIG. 6. High resolution scan of highest observed level.

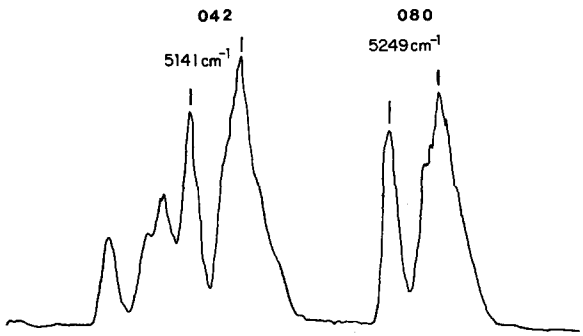

FIG. 7. High resolution scan of fourth member of the progression, pumping at 2782.22 Å.

to even higher ground state energy levels, but we were limited because of the use of the doubled YAG output for pumping the dye laser. Figure 7 shows the region near $(0,8^0,0)$. As can be seen, there is a striking hole where the states $(0,6^{0,2},1)$ should be. In retrospect, such striking intensity variations may prove useful in fine tuning the bending potential; unfortunately, the present experiments were not carried out with attention to the relative intensities, so such information would have to come from a more refined data set, including the variation in fluorescence intensity with vibrational state of the A state.

FITTING PROCEDURE

The 94 experimentally determined ground state energies were used in a least squares fitting of a rigid bender

TABLE II. Comparison of observed and calculated[a] ground state energies of HCP.

Bending state v_2^l	Stretching state (v_1, v_3) (0,0)	(0,1)	Energy[b]/cm^{-1} (0,2)	(0,3)	Obs (obs–calc)[c] (0,4)	(0,5)
0^0	[0][2]	1 279(0)	2 549(1)	3 804(−2)	[5 055]	[6 293]
1^1	[675]	1 947(1)	[3 208]	4 453(−6)	5 694(−5)	6 923(−6)
2^0	1 336(3)	2 598(1)	3 853(3)	5 097(3)	6 328(2)	[7 548]
2^2	1 364(6)	2 626(4)	3 880(4)	5 126(7)	[6 352]	[7 574]
3^1	2 002(1)	3 260(3)	4 500(−3)	5 740(1)	6 967(4)	8 180(3)
4^0	[2 652]	3 902(2)	5 141(3)	6 367(1)	[7 582]	
4^2	2 682(4)	3 932(6)	5 169(5)	6 395(3)	[7 608]	
5^1	3 309(−4)	4 537(−17)	5 778(−6)	[7 003]	8 211(−1)	
6^0	3 960(3)	[5 190]	6 411(−1)	[7 624]		
6^2	3 985(2)	[5 216]	6 440(2)	[7 650]		
7^1	4 607(−4)	5 834(−2)	7 046(−5)	8 249(−5)		
8^0	5 249(1)	6 464(−2)	[7 672]	[8 868]		
8^2	5 276(1)	6 491(−1)	[7 699]	[8 894]		
9^1	5 895(−1)	7 106(0)	8 300(−5)	9 490(−2)		
10^0	6 622(−5)	7 728(0)	[8 919]	[10 098]		
10^2	6 549(−5)	7 756(0)	[8 946]	[10 125]		
11^1	7 166(−2)	8 359(−3)	9 547(2)	10 720(4)		
12^0	[7 792]	8 981(3)	10 155(3)	[11 315]		
12^2	[7 820]	9 009(3)	10 182(2)	[11 343]		
13^1	8 424(−4)	[9 606]	10 777(5)	11 925(−2)		
14^0	9 047(1)	10 219(4)	[11 373]	[12 519]		
14^2	9 075(1)	10 247(3)	[11 402]	[12 548]		
15^1	9 680(4)	10 827(−10)	11 987(0)	13 127(3)		
16^0	10 289(2)	[11 440]	[12 851]			
16^2	10 317(1)	[11 469]	[12 610]			
17^1	10 917(6)	12 042(−13)	13 190(1)			
18^0	11 519(3)	[12 653]				
18^2	11 548(2)	[12 682]				
19^1	12 131(−3)	13 253(−10)				
20^0	12 738(5)	[13 853]				
20^2	12 766(2)	[13 884]				
21^1	13 347(1)	[14 457]				
22^0	13 942(3)	[15 042]				
22^2	13 971(0)	[15 074]				
23^1	14 547(0)	15 644(3)				
24^0	15 134(0)					
24^2	15 164(−2)					
25^1	15 736(0)					
26^0	16 317(0)					
26^2	16 347(−3)					
27^1	16 912(−1)					

[a] Energies only calculated and not observed are reported in square brackets.
[b] Energies are referred to the $(0,0^0,0)$ level of the ground state.
[c] The obs–calc values are reported in parentheses after the observed energies.

model.[15,16] The rigid bender model was modified in the manner of Ross and Bunker[17] to account for the effects of the ν_3 (C–P stretch) vibrational averaging. As no transitions involving the ν_1 vibration (C–H stretch) were seen, it is not possible to account for the effects of the ν_1 vibrational averaging solely with the present data. The effective bending potential function for the $(v_1,v_3) = (0,v_3)$ small amplitude stretching states that were observed, is [cf. Eq. (2) of Ref. 17],

$$V^{\text{eff}}_{(0,v_3)}(\rho) = V^0_{v_1=0}(\rho) + (v_3 + \tfrac{1}{2})\omega_3(\rho) + (v_3 + \tfrac{1}{2})^2 x_{33}(\rho),$$

where

$$V^0_{v_1=0}(\rho) = \tfrac{1}{2} f'_{\alpha\alpha}\rho^2 + \tfrac{1}{24} f'_{\alpha\alpha\alpha\alpha}\rho^4,$$
$$\omega_3(\rho) = \omega_3^{(0)} + \omega_3^{(2)}\rho^2,$$
$$x_{33}(\rho) = x_{33}^{(0)}.$$

$V^0_{v_1=0}(\rho)$ is thus the bending potential function corrected for the vibrational averaging of the v_3 vibration but not that of the v_1 vibration. The bending potential constants $f'_{\alpha\alpha}$ and $f'_{\alpha\alpha\alpha\alpha}$ are primed to indicate that they are to some extent "polluted" by the variation with bending angle of the v_1 stretching frequency. $\omega_3(\rho)$ is the harmonic v_3 frequency as a function of the bending angle ρ. It was sufficient to treat the x_{33} anharmonic constant as independent of the bending angle ρ.

Due to the lack of knowledge of the rotational constants for the excited vibrational states, it was not possible to determine the variation of the bond lengths with bending angle. The bond lengths that were used in the fitting were the r_e values of Strey and Mills[20]: $r_e(\text{CH}) = 1.0692$ Å, $r_e(\text{CP}) = 1.5398$ Å. These bond lengths were held fixed in the fitting.

In the least squares fitting the five parameters of the effective potential function $V^{\text{eff}}(0,v_3)(\rho)$ were simultaneously varied to fit the 94 experimentally determined ground state energies. All of the data were given equal weight. The observed-calculated differences are given in Table II and the standard deviation of the fit was 4.2 cm^{-1}, in good agreement with the estimated experimental precision. The few residuals in excess of 10 cm^{-1} probably reflect resonances to some degree; one of the most poorly fit levels is near an unassigned transition in Fig. 4.

The parameters obtained from the fitting are given in the first column of Table III. Our value for $f_{\alpha\alpha\alpha\alpha}$ represents the first reliable determination of this force constant. For comparison the values of $f_{\alpha\alpha}$ and $f_{\alpha\alpha\alpha\alpha}$ obtained by previous workers are also presented in Table III.

The dependence on bending angle of the energy of the v_3 vibration was also determined and is given by $\omega_3^{(0)}$ and $\omega_3^{(2)}$. As was the case for the HCN/CNH study,[17] the dependence of x_{33} on bending angle was not determined. Cabana *et al.*[11] obtained a somewhat different x_{33} from ours. The size of this discrepancy is in line with previous comparisons[17] and probably results from the larger amount of experimental vibrational data, although of lower accuracy, that was at our disposal.

The value of $f_{\alpha\alpha}$ given in the first column of Table II is corrected for the v_3 vibrational averaging, through $\omega^{(2)}$, but not for the v_1 vibrational averaging. To estimate the effect of the v_1 vibrational averaging on the potential function, the three observed vibrational states[11] involving v_1, (1, 0^0, 0), (1, 1^1, 0) and (2, 0^0, 0), were used to determine the three v_1 vibrational constants $\omega_1^{(0)}$, $\omega_1^{(2)}$, and x_{11}, while keeping all other constants fixed. The resulting value for $f_{\alpha\alpha}$ corrected now for both v_1 and v_3 vibrational averaging, is given in the second column of Table III. Also given are the v_1 vibrational constants. Because these constants result from a "perfect fitting," three data fitted with three constants, their errors could not of course be determined, and their final values are very sensitive to any perturbations in the observed levels.

The resulting true bending potential is shown as a function of the bending angle ρ by the solid curve in Fig. 9. The horizontal line at 17 500 cm^{-1} approximately corresponds to the highest observed bending energy, including the zero point, and thus indicates the region over which the potential function is determined, viz., 0°–100°. Although the highest

TABLE III. Parameters of the rigid bender model obtained by the least squares fitting. aJ = 10^{-18} J.

Parameter	Present work		Reference 20	Reference 21
$f_{\alpha\alpha}$/aJ rad^{-2}	0.247 97(12)[a,b]	0.2595[c]	0.2550	0.255
$f_{\alpha\alpha\alpha\alpha}$/aJ rad^{-4}	− 0.097 76(69)[b]		0.05[d]	0.3
$\omega_1^{(0)}$/cm^{-1}		3339.1[e]		
$\omega_1^{(2)}$/cm^{-1} rad^{-2}		− 231.0[e]		
$\omega_3^{(0)}$/cm^{-1}	1296.7(13)			
$\omega_3^{(2)}$/cm^{-1} rad^{-2}	− 136.6 (11)			
			Ref. 11	
$x_{11}^{(0)}$/cm^{-1}		− 55.6961[e]	− 55.6961(39)	
$x_{33}^{(0)}$/cm^{-1}	− 5.08 (24)		− 5.6751 (56)	

[a] The number in parentheses is one standard deviation in units of the last digit quoted for the parameter.
[b] These values are uncorrected for the ν_1 vibrational averaging. These are the values for $f'_{\alpha\alpha}$ and $f'_{\alpha\alpha\alpha\alpha}$.
[c] This value has been corrected for the estimated effect of the ν_1, vibrational averaging. See the text for an explanation.
[d] These authors use a definition of $f_{\alpha\alpha\alpha\alpha}$ different from the usual one. The value reported here has been converted to the usual definition.
[e] Estimated values, see the text.

observed bending state lies slightly above the energy needed to isomerize HCN into CNH ($\sim 17\,300\ cm^{-1}$)[14] the empirical HCP bending potential shows no sign of turning over to form a minimum for CPH. Thus the bending potentials of HCN and HCP are quite different, despite the close similarity in most other spectroscopic properties.

A semirigid bender fitting was also done, using bond lengths determined by fitting our *ab initio* values (Table V and Fig. 8) for values of ρ from 0° to 75° to give $r_{HC} = (1.0619 + 0.0176\ \rho^2)$ Å, $r_{CP} = (1.5149 + 0.0311\ \rho^2)$ Å. The resulting potential function agrees to within better than 200 cm^{-1} with the one determined by the rigid bender fitting. We thus anticipate that the error introduced by the assumption of a rigid bending geometry to be on the order of 1%.

AB INITIO CALCULATIONS

In the first part of a recent theoretical study[22–25] of the gas-phase proton affinities of molecules containing P–C or As–C multiple bonds, there was noted a striking difference between HCN and HCP, namely, that while the former protonates at N to form the linear $HCNH^+$, the latter protonates at C to form the planar H_2CP^+. The linear molecule $HCPH^+$ was found not only to lie much higher in energy than planar H_2CP^+ (approximately 185 kJ mol^{-1} in the most accurate calculations which were reported, namely those at the MP 4/6-31G**//HF/6-31G* level described below), but also to be a local energy *maximum* with respect to one degenerate pair of bending modes. This contrast in behavior between protonated HCN and HCP seems in line with what the experimental results imply about the difference in bending potentials between HCN and HCP. It was therefore decided to compute an *ab initio* bending potential over the full range of bending angle going from HCP to CPH.

COMPUTATIONAL METHODS

Bond lengths corresponding to a semirigid bender model of the HCP–CPH system were obtained by optimization using energy gradients at the SCF (single determinantal) level, the GAUSSIAN 80 program,[26] and the split-valence plus polarization basis set[27,28] 6-31G* (polarization functions used for P and C only). The computational level is designated as HF/6-31G*. All six $(s + d)$ second-order Gaussian polarization functions were used for both the P and C atoms. Specifically the H–C and C–P bond lengths were optimized for values of ρ, defined as 180° minus the H–C–P bond angle, ranging from 0°(HCP) to 180°(CPH), with the H–P bond distance then being computed geometrically. The computed H–C and C–P equilibrium distances for linear HCP, namely 1.063 and 1.515 Å, respectively, are close to the r_e values of 1.0692 and 1.5398 Å determined by Strey and Mills[20] fit to the experimental results. Detailed theoretical studies of the HCP bond lengths have been reported by Thompson and Ellam.[29] A theoretical determination of the HCP stretching potential in the linear geometry has been reported by Botshwina and Sebald.[30]

For each of the optimized geometries (Table IV) the energy was recomputed at the MP4SDQ level (fourth-order Møller-Plesset perturbation theory with single, double, and quadruple excitations from a single reference configuration) using the 6-31G** basis set, identical to 6-31G* except that p-type polarization functions for the H atom have been included. The resulting energies and energy differences, designated as MP4SDQ/6-31G**//HF/6-31G*, are also given in Table IV. This is a computational level which we have found to give a very satisfactory description of the proton affinities of PH_3, HCP, H_2CPH, and H_3CPH_2, as well as of the $HCPH^+$–H_2CP^+ isomerization energy.[22–25] In computing the MP 4SDQ correlation corrections the inner shells (1s for C and 1s, 2s, and 2p for P) were excluded. Finally, vibrational frequencies were calculated (Table V) for HCP and CPH

TABLE IV. *Ab initio* structures, overlap populations, and energies for HCP/CPH.

	Interatomic distances (Å)			Overlap populations[d]			MP4SDQ/6-31G**//HF/6-31G* energies	
ρ[a]	H–C[b]	C–P[b]	H–P[c]	H–C	C–P	H–P	E (a.u.)	ΔE (cm^{-1})
0 (HCP)	1.063	1.515	2.578	0.962	1.746	−0.056	−379.366 29	0
15	1.064	1.517	2.559	0.957	1.729	−0.058	−379.364 18	463
30	1.066	1.523	2.504	0.728	1.686	−0.064	−379.357 82	1 858
45	1.071	1.534	2.413	0.744	1.620	−0.070	−379.347 20	4 189
60	1.079	1.549	2.288	0.752	1.524	−0.074	−379.332 19	7 482
75	1.094	1.568	2.132	0.730	1.394	−0.066	−379.312 91	11 713
90	1.123	1.587	1.944	0.639	1.254	−0.032	−379.292 25	16 247
105	1.185	1.594	1.722	0.442	1.162	0.056	−379.278 72	19 216
120	1.360	1.608	1.499	0.170	1.109	0.243	−379.272 51	20 578
135	1.978	1.640	1.419	0.015	1.090	0.528	−379.258 54	23 644
150	2.533	1.648	1.379	−0.019	1.153	0.642	−379.247 95	25 967
165	2.866	1.603	1.381	−0.021	1.336	0.637	−379.237 76	28 204
180 (CPH)	2.961	1.576	1.385	−0.018	1.498	0.621	−379.232 32	29 397

[a] $\rho \equiv 180° - \Theta$, where Θ is H–C–P angle in degrees.
[b] Distances optimized at HF/6-31G* level for fixed ρ.
[c] Distance computed from H–C and C–P distances for given ρ.
[d] HF/6-31G**//HF/6-31G* level.

TABLE V. Comparison of calculated[a] and observed[b] vibrational frequencies.[c]

Mode	Symmetry	HCP		HPC	
		Calc.	Obs.	Calc.	Obs.
$\bar{\nu}_1$	σ^+	3578	3216.89	2722	...
$\bar{\nu}_2$	π	830	674.70	645i[d]	...
$\bar{\nu}_3$	σ^+	1472	1278.28	1311	...

[a] HF/6-31G* level.
[b] Reference 11.
[c] In cm^{-1}.
[d] Imaginary frequency.

using analytical second derivatives[31] at the HF/6-31G* level and the GAUSSIAN82 program.

RESULTS AND DISCUSSION

The HF/6-31G* bond lengths are given in Table IV and in Fig. 8 as a function of the angle ρ. We note a transition region from $\rho = 105°$ to 135° characterized by a transfer of H from C to P. This transfer is also seen in the overlap populations (Table IV) calculated at the HF/6-31G**//HF/6-31G* level. We note that the transfer region has a smaller C–P overlap population and a longer C–P bond than either HCP or CPH. A similar transition region occurs at the top of the isomerization barrier in the HCN/CNH system.[14] However in HCP the transition region does not correspond to a local energy maximum, the usual sense of a transition state, but instead corresponds to an energy shoulder or more figuratively an alpine meadow. Indeed our most striking result given by the MP4SDQ/6-31G**//HF/6-31G* energies (Table IV and Fig. 9), as well as the HF/6-31G* vibrational frequencies (Table V), is that the linear structure of CPH corresponds to a local energy *maximum*, with the structure being unstable with respect to the degenerate bending mode. This instability may be described as a second-order Renner effect, in which the Σ ground state of CPH is mixed by the π bending mode with a π excited electronic state. This is similar to the instability in isoelectronic linear $HCPH^+$ discussed previously. Both CPH and $HCPH^+$ have low-lying empty σ^* MO's to which excitation from occupied π MO's yield $^1\pi$ and $^3\pi$ multiplets. Although not corresponding to the spectroscopic energy differences $E(^1\pi) - E(^1\Sigma)$, the orbital energy differences $\Delta\epsilon = \epsilon(\sigma^*) - \epsilon(\pi)$ are revealing; at the HF/6-31G* level $\Delta\epsilon$'s are 16.52, 12.16, and 13.32 eV for HCP, CPH, and $HCPH^+$, respectively, indicating much smaller excitation energies for CPH and $HCPH^+$ than for HCP.

Figure 9 displays the MP4SDQ/6-31G**//HF/6-31G* energies vs ρ. The energies are somewhat dependent on the computational level. Specifically the E(CPH)–E(HCP) differences obtained with the 6-31G** basis set and the HF/6-31G* geometries are 29 397, 31 004, and 32 660 cm^{-1}, at the MP4SDQ, MP3, and HF levels, respectively, indicating the role of electron correlation in lowering the difference.

Also plotted in Fig. 9 is the experimentally determined bending potential over the range in which the experimental results span. As can be seen, the agreement is excellent. It is seen that the calculated potential, like the experimentally determined one, is surprisingly parabolic for bending vibrational energies up to approximately 17 000 cm^{-1}.

As mentioned before, Table V lists vibrational frequencies calculated from analytical second derivatives at the HF/6-31G* level. The values for HCP are approximately 12% to 20% higher than the observed[11] values. This is the same level of agreement noted[32] by Pople *et al.* in a comparison of HF/6-31G* and observed frequencies for a large number of molecules including HCN, for which the calculated frequencies

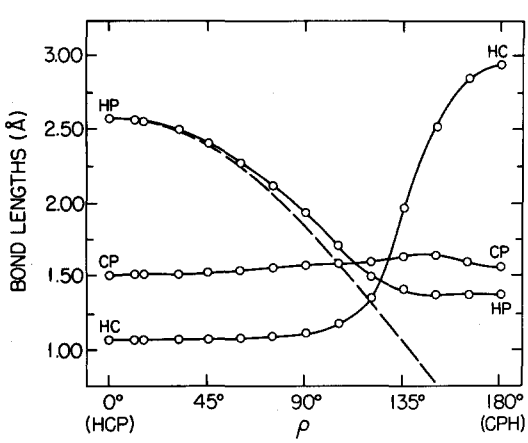

FIG. 8. Optimized values at the HF/6-31G* level for the CP and CH distances in Å in HCP as a function of the angle ρ defined as 180° − ∠HCP. The resulting HP distances are also shown together with their values (dashed line) in a rigid bender model in which the CP and HC distances are held at their values for $\rho = 0$.

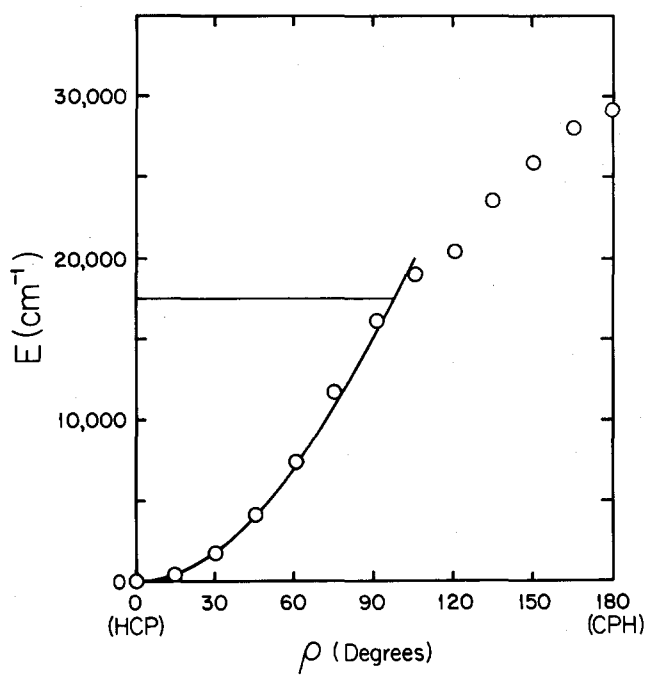

FIG. 9. Comparison of *ab initio* energies (open circles), in cm^{-1}, at the MP4DSQ/6-31G**//HF/6-31G* level with the experimentally determined bending potential (solid curve). The horizontal line at 17 575 cm^{-1} denotes the highest observed energy level. The bending angle ρ is 180° minus the H–C–P angle.

are 3679, 889, and 2438 cm^{-1}, as compared to observed values[17] of 3311, 713, and 2097 cm^{-1} for ν_1, ν_2, and ν_3, respectively. The key present results are not only that ν_1 and ν_3 are somewhat less for CPH than for HCP, but also that ν_2 is imaginary (negative force constant) for CPH. These calculated frequencies correspond to ZPE's of 40.1 and 24.1 kJ mol^{-1} for HCP and CPH, respectively. As HCP has the higher ZPE, the E(CHP)–E(HCP) values should be reduced by an amount not greater than the difference in ZPE values of 16 kJ mol^{-1} (1337 cm^{-1}) based upon our calculated vibrational frequencies. The instability of CPH with respect to the bending mode has already been discussed in terms of the energies in Table IV and Fig. 9. We note here that the displacement variable for the CPH bending frequency is the H–P–C angle, which differs from ρ used in Table IV and Fig. 9, although the instability of linear CPH is manifested in either variable.

The energy for CPH relative to HCP, namely 351.7 kJ mol^{-1} or 29 420 cm^{-1} at the MP4SDQ/6-31G**//HF/6-31G* level is nearly twice the 184.8 kJ mol^{-1} difference between $HCPH^+$ and H_2CP^+ calculated at the same level. The smaller isomerization energy for H_2CP^+ as compared to HCP is in large part a reflection of the approximately 200 kJ mol^{-1} required to bend HCP to an H–C–P angle of 122° ($\rho = 58°$), corresponding to the computed HF/6-31G* value of the angle in H_2CP^+.

DISCUSSION AND CONCLUSIONS

There are several quite significant results of this study, and we would like to take this opportunity to discuss them.

First, the observation of photochemical activity of HCP, discovered accidentally and not pursued, opens this new class of novel compounds up for the possibility of further new chemistry.

Second, the fluorescence lifetime measurements confirm some of the speculations of the previous high resolution UV work of Johns *et al.*[2] Further study, such as Stark and Zeeman quantum beats may better characterize these excited electronic states.

Third, the determination of 94 vibrational energy levels, combined with the previously measured IR vibrational states means that more vibrational states are known for HCP than have been reported for even HCN and H_2O. Johns *et al.*'s study characterized more excited electronic states than any other polyatomic molecule,[1] so HCP may now be the most spectroscopically characterized polyatomic molecule, despite its chemical obscurity and the lack of thermodynamic data.

Fourth, the observed vibrational energy levels have been fit to experimental accuracy (5 cm^{-1}) by a rigid bender Hamiltonian with only five adjustable parameters. This model has determined the bending potential of HCP over a range of angles from 0°–100°, a range unprecedented for any rigid triatomic molecule. The bending potential is found to be described over that range by only two parameters, a quadratic term and a small quartic term. The variation of the C–P stretching frequency with bending angle, as well as its anharmonic constant x_{33} have also been determined.

The success of the rigid bender Hamiltonian in fitting the HCP data is striking when one remembers the essential 2-1 resonance between the bending mode and the C–P stretch that pervades the entire range of observed energy levels. The rigid bender Hamiltonian uses an adiabatic separation to remove the small amplitude stretching degrees of freedom and so is not expected to be able to treat bend–stretch resonances directly. However, the C–P stretching vibration ν_3 decreases with increasing excitation of the bending mode, faster than the anharmonicity of the bending mode decreases its vibrational intervals. Therefore, the 2-1 resonance between ν_2 and ν_3 detunes with increasing excitation in ν_2.

The recent chemical physics literature has been overwhelmed with descriptions of how delocalized or chaotic such highly excited vibrational states should be. The apparent simplicity of most high overtone states has recently been attributed to the peculiar character of those states, having all the action localized in one mode.[33] The excited vibrational states observed here have their action spread over two modes, three if you count the l quantum number. Thus the simplicity of their spectrum, explainable in terms of separable modes of vibration, stands in even sharper contrast to the expected delocalized behavior. It must be pointed out that the approximately 10 cm^{-1} resolution of this experiment does not rule out that the states are delocalized, as long as the relaxation rate from the zero order state is not greater than 300 GHz. Still, this is approaching time scales for which nonstatistical chemical behavior would be expected.

Fifth, the *ab initio* calculations that have been performed on HCP are in excellent agreement with this and previous known spectroscopic data on this molecule. The *ab initio* bending potential is in excellent agreement with the experimentally determined potential over the latter's range of validity. Therefore, the conclusions of the *ab initio* calculation, that CPH is unbound, being a saddle point ~30 000 cm^{-1} higher in energy than HCP, can be accepted with confidence. This points out once again that the chemistry of the C≡P group, though analogous to that of C≡N, has many of its own peculiarities that will be revealed now that its study has begun in earnest by groups such as Kroto's.[34]

ACKNOWLEDGMENTS

The experimental work reported in this paper was performed at the MIT Regional Laser facility. KKL would like to thank that facility for allowing him its use, and Dr. Carter Kitrell and Dr. George J. Scherer for help in setting up the experiment. Gilbert Nathanson's help with preliminary steps of the experiment is appreciated. Patrick Vaccaro provided programs for lifetime measurement and fitting, and detailed help in learning to use the programs. Professors Robert W. Field and Professor William Klemperer provided equipment, supplies, encouragement, and advice. The Harvard Milton Fund provided funds for conducting the experiment. SR would like to thank Dr. F. W. Birss for many late night discussions and his generous support from a grant awarded by the Natural Sciences and Engineering Research Council of Canada. LLL would like to thank the Computing Center of the University of Michigan for the use of its Adahl 470V/8 computer and Professor H. B. Schlegel for many

helpful suggestions and for calculation the HCP vibrational frequencies.

[1]K. K. Innes in *Molecular Spectroscopy: Modern Research*, edited by K. N. Roa and C. W. Mathews (Academic, New York, 1972).
[2]J. W. C. Johns, H. F. Shurvell, and J. K. Tyler, Can. J. Phys. **47**, 893 (1969).
[3]A. Hartford, J. G. Moehlmann, and J. R. Lombardi, J. Chem. Phys. **56**, 5733 (1972).
[4]D. C. Frost, T. Lee, and C. A. McDowell, Chem. Phys. Lett. **23**, 472 (1973).
[5]M. A. King, H. W. Kroto, J. F. Nixon, D. Klapstein, J. D. Mairer, and O. Marthalen, Chem. Phys. Lett. **82**, 543 (1981).
[6]J. K. Tyler, J. Chem. Phys. **40**, 1170 (1964).
[7]J. W. C. Johns, J. M. R. Stone, and G. Winnewisser, J. Mol. Spectrosc. **38**, 437 (1971).
[8]J. M. Garneau and A. Cabana, J. Mol. Spectrosc. **69**, 319 (1978).
[9]J. M. Garneau and A. Cabana, J. Mol. Spectrosc. **79**, 502 (1980).
[10]J. M. Garneau and A. Cabana, J. Mol. Spectrosc. **87**, 490 (1981).
[11]A. Cabana, Y. Doucet, J. M. Garneau, C. Pepin, and P. Puget, J. Mol. Spectrosc. **96**, 342 (1982).
[12]G. Hertzberg and K. K. Innes, Can. J. Phys. **35**, 842 (1957).
[13]C. F. Pau and W. J. Hehre, J. Phys. Chem. **86**, 321 (1982).
[14]P. K. Pearson, H. F. Schaefer, and U. Wahlgren, J. Chem. Phys. **62**, 350 (1975).
[15]J. T. Hougen, P. R. Bunker, and J. W. C. Johns, J. Mol. Spectrosc. **34**, 136 (1970).
[16]P. R. Bunker and J. M. R. Stone, J. Mol. Spectrosc. **41**, 310 (1972).
[17]S. C. Ross and P. R. Bunker, J. Mol. Spectrosc. **101**, 199 (1983).
[18]M. J. Hopkinson, H. W. Kroto, J. F. Nixon, and N. P. C. Simmons, J. Chem. Soc. Chem. Commun. **513**, (1976).
[19]J. G.Moehlmann, A. Hartford, and J. R. Lombardi, Can. J. Phys. **50**, 1705 (1972).
[20]G. Strey and I. M. Mills, Mol. Phys. **26**, 129 (1973).
[21]J. N. Murrell, S. Carter, and L. P. Halonen, J. Mol. Spectrosc. **93**, 307 (1982).
[22]L. L. Lohr, H. B. Schlegel, and K. Morohuma, J. Phys. Chem. **88**, 1981 (1984).
[23]L. L. Lohr and S. H. Ponas, J. Phys. Chem. **88**, 2992 (1984).
[24]L. L. Lohr and A. C. Scheiner, J. Mol. Struct. Theochem. **101**, 195 (1984).
[25]L. L. Lohr, J. Phys. Chem. **88**, 3607 (1984).
[26]J. S. Binkley, R. A. Whiteside, R. Krishman, R. Seeger, D. J. DeFrees, H. B. Schlegel, S. Topiol, L. R. Kahn, and J. A. Pople, QCPE **13**, 406 (1980).
[27]R. C. Hariharan and J. A. Pople, Theor. Chim. Acta **28**, 213 (1973).
[28]M. M. Franel, W. J. Pietro, W. J. Hehre, J. S. Binkley, M. S. Gordon, and D. J. DeFrees, J. Chem. Phys. **77**, 3654 (1982).
[29]C. Thompson and P. Ellam, Theor. Chim Acta **62**, 81 (1982).
[30]P. Botschwina and P. Sebald, J. Mol. Spectrosc. **100**, 1 (1983).
[31]J. A. Pople, R. Krishnan, H. B. Schlegel, and J. S. Binkley, Int. J. Quantum Chem. Symp. **13**, 225 (1982).
[32]J. A. Pople, H. B. Schlegel, R. Krishnan, D. J. DeFrees, J. S. Binkley, M. J. Frish, R. A. Whiteside, R. J. Hont, and W. J. Hehre, Int. J. Quantum Chem. Symp. **15**, 269 (1981).
[33]G. Hose and H. S. Taylor, Chem. Phys. **84**, 375 (1984).
[34]H. W. Kroto, Chem. Soc. Rev. **11**, 435 (1982).